

Reductions of 1,3,5-Triboracyclohexanes and Related 1,3,5-Triboraalkanes with Alkali Metals to Trishomoaromatic Aggregates — Tetrameric Lithium and Sodium, and Polymeric Sodium and Potassium Trishomoaromatic Cyclotriborate Compounds

Wolfgang Löblein,^[a] Hans Pritzkow,^[a] Paul von Ragué Schleyer,^{*[b]} Lawrence R. Schmitz,^[c] and Walter Siebert^{*[a]}

Dedicated to Prof. Kurt Dehnicke on the occasion of his 70th birthday

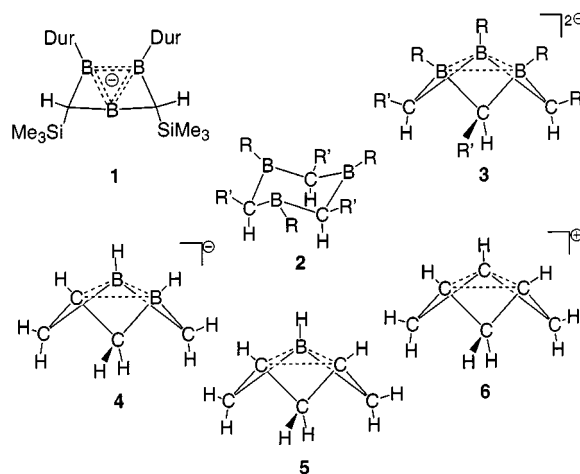
Keywords: Boron / Aromaticity / NMR spectroscopy / Alkali metals

Hexamethyl-1,3,5-triboracyclohexane can be reduced by alkali metals in donor solvents. Two electrons are added to the combination of p-orbitals at the boron centers forming trishomoaromatic dianions. X-ray structure analyses show a variety of arrangements, depending on the alkali metal: Tetrameric aggregates with lithium, a polymeric, meander-like chain or a complex tetramer with sodium, and a zigzag-chain polymer with potassium. The set of dianions show characteristic NMR chemical shifts in the high-field region, but do not

obey a monotonous order with the counterions Li^+ to Cs^+ . Lithium is out of line because of its exceptionally low electronegativity. IGLO chemical shift calculations agree very well with the experimentally observed data. The computed Nucleus-Independent Chemical Shift (NICS) values prove the strong homoaromatic character of the reduced triboraheterocycles. Compared with isoelectronic analogues the reduced triboraheterocycle shows a remarkable stabilization energy towards the corresponding, non-aromatic species.

Introduction

Reduction of unsaturated boron heterocycles in donor solvents by alkali metals leads to the formation of aromatic anions.^[1] Remarkable results such as the synthesis of the doubly-aromatic anion **1** with σ and π 3c,2e bonding have been reported by Berndt et al.^[2,3] Recently we obtained the new, trishomoaromatic system **3** by reducing 1,3,5-triboracyclohexanes **2** with lithium.^[4,5] The empty p-orbitals of **2** are able to accept two electrons to form the dianion **3**, which is isoelectronic with the trishomocyclopropenylum cation **6**.^[6] We now describe the reactions of the hexamethyl derivative **2** with various alkali metals and the influence of these metals on the structures and on the NMR chemical shifts of the trishomoaromatic dianions **3**. Our investigations are supported by computational studies on the stabilization and on the Nucleus-Independent Chemical Shifts (NICS)^[7] of the isoelectronic, parent trishomoaromatic set **4**, **5**, and **6**.



Results and Discussion

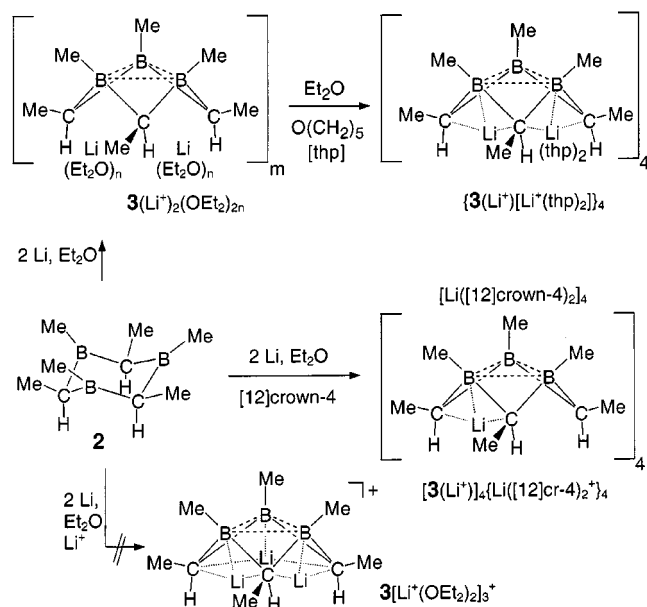
Formation and X-ray Structure Analyses of Trishomoaromatic Dianions

Hexamethyl-1,3,5-triboracyclohexane (**2**) reacted with Li powder at 0 °C in both Et_2O and THF (Scheme 1) to give yellow-orange solutions after filtration. Removal of the solvent gave only amorphous products $\{3[(\text{Li}^+)_2(\text{OEt}_2)_{2n}]\}_m$ and $\{3[(\text{Li}^+)_2(\text{thf})_{2n}]\}_m$ of unknown structure.

^[a] Anorganisch Chemisches Institut der Universität, Im Neuenheimer Feld 270, 69120 Heidelberg

^[b] Computational Chemistry Annex, Department of Chemistry, University of Georgia, Athens, GA, 30602 USA

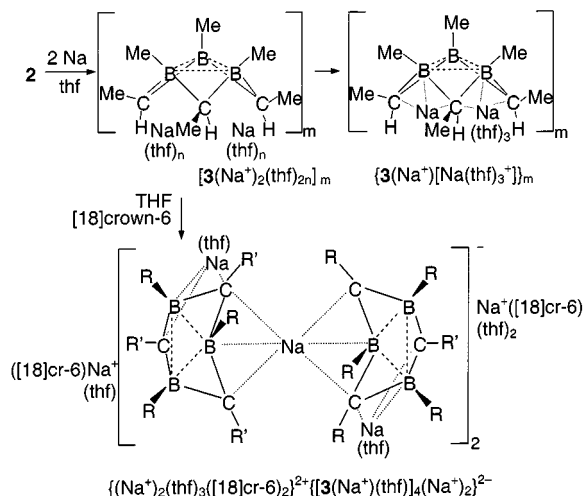
^[c] Marshall University, 400 Hal Greer Blvd, Huntington, WV, 25755 USA



Scheme 1

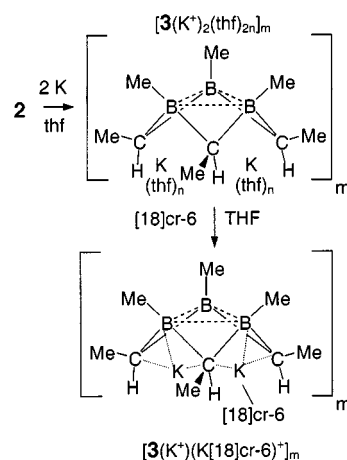
Very air- and moisture-sensitive crystals were obtained by adding tetrahydropyran (thp) or [12]crown-4 to THF solutions of reduced **2**. Surprisingly, the X-ray structures (see below) revealed tetrameric aggregates for $\{3(\text{Li}^+)-[\text{Li}(\text{thp})_2]^+\}_4$ and for $\{3(\text{Li}^+)_4[\text{Li}([12]\text{cr-4})_2]^+\}_4$. The low solubility of both these compounds precluded spectroscopic characterization. An attempt to obtain $3[\text{Li}(\text{OEt}_2)_2]_3^+$ by reducing **2** with lithium in Et_2O in the presence of LiCl failed to give any monomeric product.

To study the reaction with the other alkali metals **2** was treated with sodium, potassium, rubidium, or cesium as described above (Scheme 2–4). The initially formed amorphous reduction products were soluble in $[\text{D}]_8\text{THF}$.

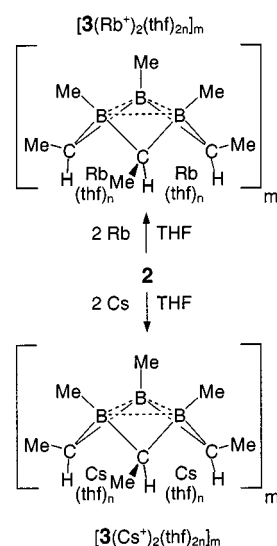


Scheme 2. Reduction of **3** with sodium; in the formula of $\{(\text{Na}^+)_2(\text{thf})_3([18]\text{cr-6})_2\}^{2+}\{[3(\text{Na}^+)(\text{thf})_4(\text{Na}^+)_2]^{2-}\}$ the hydrogen atoms are omitted

The reduction of **2** with sodium or potassium gave crystals in addition to the amorphous products. X-ray structure



Scheme 3



Scheme 4

analyses revealed a polymeric aggregation of $3(\text{Na}^+)_2(\text{THF})_3$ and, in the presence of [18]crown-6, an interesting tetramer. In contrast the potassium structure forms only a zigzag polymer (see below). The X-ray structures of all the reduced **2** products reveal that they adopt *nido* arrangements with axial methine hydrogens and equatorial CH_3 groups.

For $[3(\text{Li}^+)\text{Li}(\text{thp})_2]_4$ only a very limited data set ($2\theta_{\text{max}} = 30^\circ$) was obtained. However, the structure could be solved and showed severe disorder of the thp ligands; a gross description of the structure (Figure 1) can therefore be given. The structure of $[3(\text{Li}^+)_4\{\text{Li}([12]\text{cr-4})_2\}^+]_4$ with [12]crown-4 as ligand refined well (Figure 2). In both structures four $(\text{MeCH})_3(\text{MeB})_3$ units in the cyclic tetramer are connected by Li cations. While the second Li of each dianion in $[3(\text{Li}^+)\text{Li}(\text{thp})_2]^+$ is capping the third C_2B plane, in $[3(\text{Li}^+)_4\{\text{Li}([12]\text{cr-4})_2\}^+]_4$ the second Li is completely separated from the dianion **3** by two crown ether ligands leaving the third C_2B plane uncoordinated. The boron–boron distances in the B_3 ring are larger than $2c, 2e$ B–B bonds and differ somewhat [1.825(5) Å when both B atoms coordinate to Li's, vs. 1.851(5) and

1.848(5) Å, when only one B coordinates to Li]. The Li...B contacts are long [2.239(6) and 2.251(6) Å] and the B–C bond lengths are normal for a single bond [between 1.603(5) and 1.632(4) Å]. In $[3(\text{Li}^+)]_4[\text{Li}(\text{[12]cr-4})_2]^+$ the axial hydrogen substituents could be located.

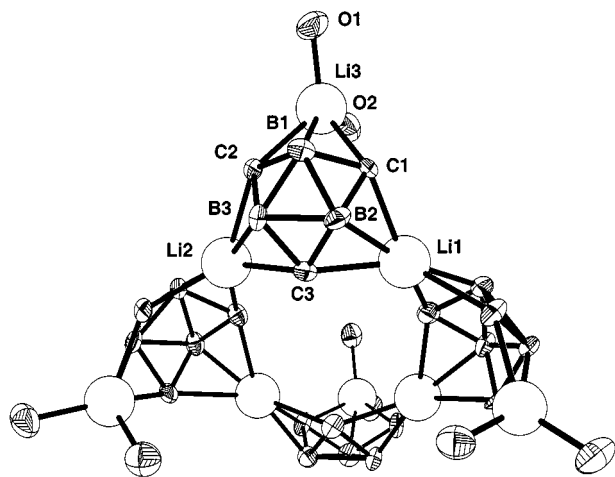


Figure 1. Structure of $\{3(\text{Li}^+)[\text{Li}(\text{thp})_2]^+\}_4$ in the crystal [the $(\text{CH}_2)_4$ chain of the thp ligands and the methyl groups are omitted for clarity]

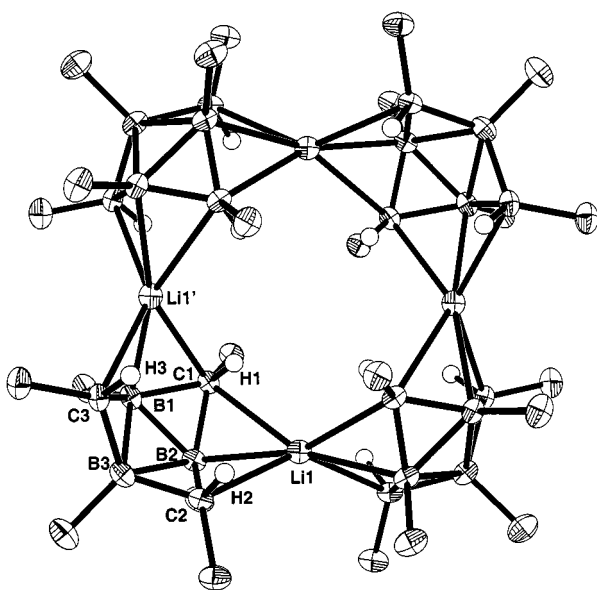


Figure 2. Molecular structure of the tetrameric anion in $\{3(\text{Li}^+)[\text{Li}(\text{[12]cr-4})_2]^+\}_4$ in the crystal; selected distances [Å] and angles [°]: B1–B2 1.825(5), B1–B3 1.851(5), B2–B3 1.848(5), Li1–C1 2.456(6), Li1'–C1 2.354(6), Li1'–C3 2.285(6), Li1–C2 2.247(6), Li1'–B1 2.239(6), Li1–B2 2.251(6); B2–B1–B3 60.4(2), B1–B2–B3 60.5(2), B1–B3–B2 59.1(2), B1–C1–B2 68.6(2), B2–C2–B3 70.0(2), B1–C3–B3 69.8(3) (symmetry operation for ' : y, 3/2 – x, 1/2 – z)

Air- and moisture-sensitive crystals of $\{3(\text{Na}^+)(\text{thf})_3\}_m$ were obtained after partial removal of the THF solvent. Surprisingly, the X-ray structure analysis (Figure 3a,b) revealed a polymeric arrangement of $\{3(\text{Na}^+)[\text{Na}(\text{thf})_3]^+\}_m$, consisting of a two-dimensional, meander-like chain pattern. There is no contact between

individual chains. Half of the sodium centers bridge the 3 units through C_2B interactions and are solvent free; the other sodium centers in the terminal positions are coordinated by three THF ligands.

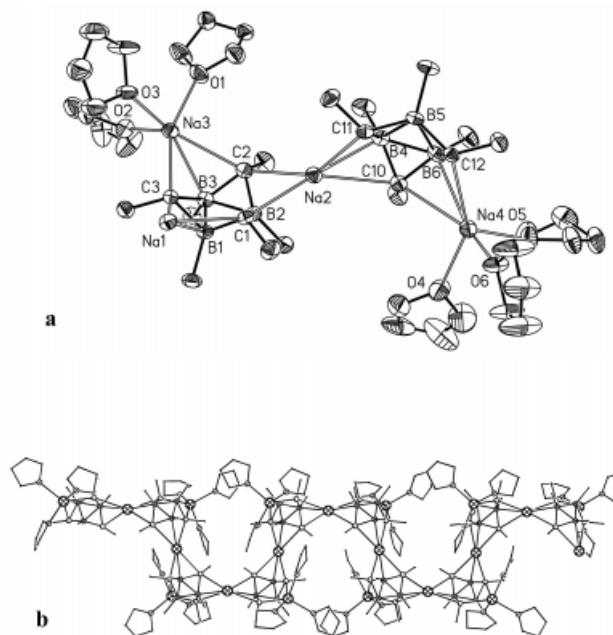


Figure 3. (a) Structure of two units of $\{3(\text{Na}^+)[\text{Na}(\text{thf})_3]^+\}_m$ in the crystal; selected distances [Å] and angles [°]: B–B 1.827–1.846(6), Na1(2)–B 2.447–2.471(5), Na1(2)–C 2.621–2.764(5), Na3–B3 2.595(5), Na4–B6 2.601(6), Na3–C 2.673(4), 2.827(5), Na4–C 2.689(4), 2.768(5), Na3(4)–O 2.316–2.360(4); B–B–B 59.6–60.7(3), B–C–B 68.2–69.5(3); (b) structure of the meander-like chain of $\{3(\text{Na}^+)[\text{Na}(\text{thf})_3]^+\}_m$ in the crystal

A few crystals could be obtained when an excess of [18]crown-6 was added to the solution of the Na-reduced ring. An X-ray structure analysis showed tetrahedral aggregation of four units of 3 around an octahedron of six sodium ions, each connecting two C_2B faces of adjacent dianions of 3. Four of the six sodium ions are complexed by a THF ligand, while the remaining two *trans*-oriented Na^+ ions have no other contacts than to the two adjacent C_2B units in 3. In the crystal these two Na ions are shielded by a $\{(\text{thf})_2\text{Na}(\text{[18]cr-6})\}^+$ unit and a $\{(\text{thf})\text{Na}(\text{[18]cr-6})\}^+$ unit, which balance the charge of the tetrameric dianion (Figure 4 and 5).

Unfortunately, no NMR spectroscopic data could be obtained. The “vacant” coordination site of $\{(\text{thf})\text{Na}^+(\text{[18]cr-6})\}^+$ is involved in an agostic interaction with a methyl group of 3 (dashed line in Figure 5). Disorder decreases the quality of the X-ray structure analysis.

The addition of [18]crown-6 after reduction of 2 with potassium yielded crystals. One of the K^+ ions bridges the C_2B faces of two adjacent units 3 resulting in a zigzag chain (Figure 6 and 7). The other K^+ ion occupies the third face of 3 and is coordinated by [18]cr-6.

In the structures the bond lengths and angles within 3 are almost identical. Due to the growing ionic radii from Li^+ to K^+ the distances of the cations to the C_2B faces

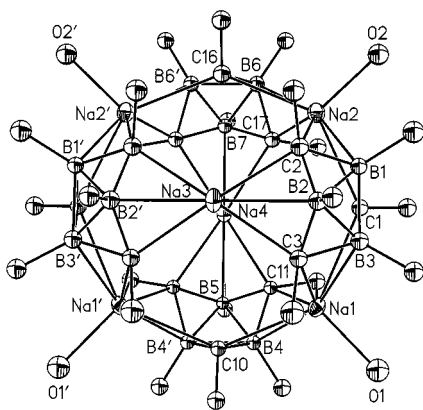


Figure 4. Structure of the dianion of compound $\{(\text{thf})_2\text{Na}([18]\text{cr-6})\}^+ \{[3(\text{Na}^+)(\text{thf})_4(\text{Na}^+)_2]\}^{2-} \{(\text{thf})\text{Na}([18]\text{cr-6})\}^+$ in the crystal (symmetry operation for ' : $x, y, -z$)

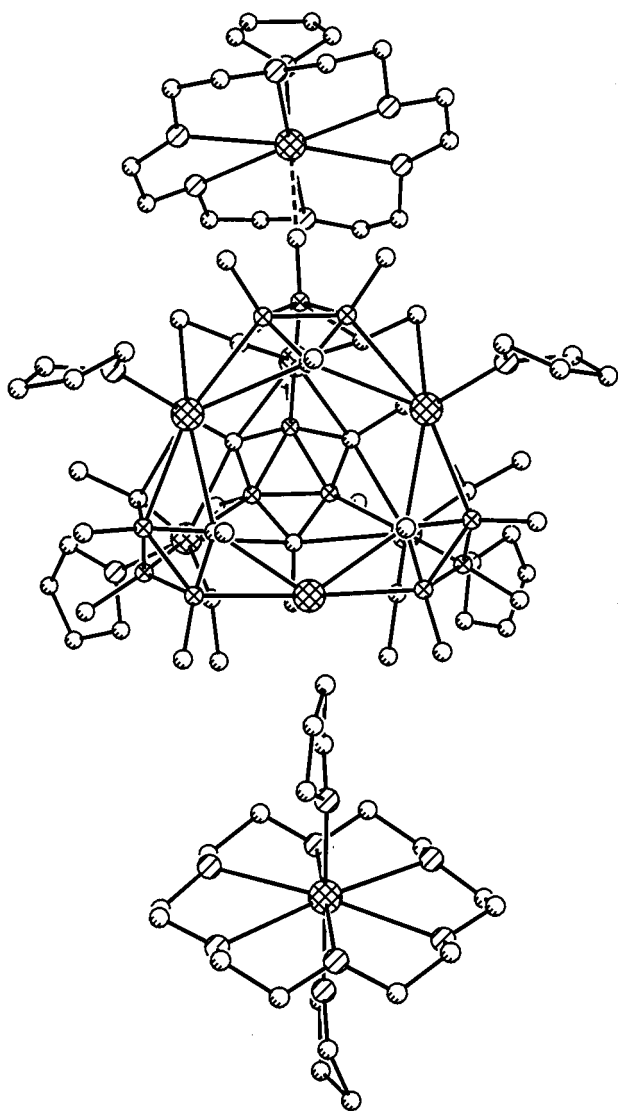


Figure 5. Molecular structure of $\{(\text{thf})_2\text{Na}([18]\text{cr-6})\}^+ \{[3(\text{Na}^+)(\text{thf})_4(\text{Na}^+)_2]\}^{2-} \{(\text{thf})\text{Na}([18]\text{cr-6})\}^+$ in the crystal

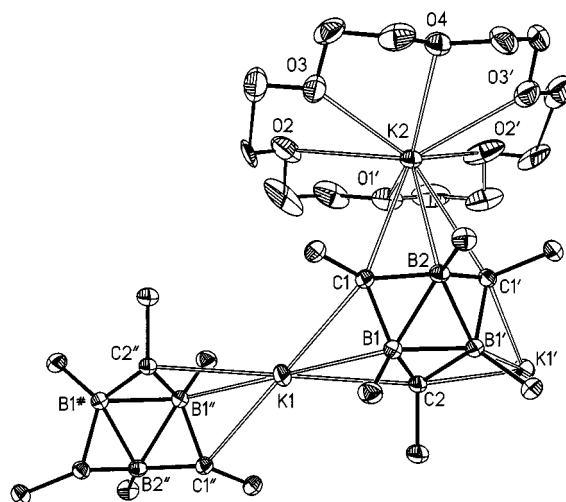


Figure 6. Structure of two units of $[3(\text{K}^+)(\text{K}[18]\text{crown-6})^+]_m$ in the crystal (one $(\text{K}^+([18]\text{cr-6}))$ unit omitted for clarity); selected distances [Å] and angles [°]: B1–B2 1.868(4), B1–B1' 1.831(5), K1–B1 2.798(3), K2–B2 3.147(3), K1–C1 2.944(2), K1–C2 2.978(1), K2–C1 3.164(2), K2–O 2.893–3.002(5); B1'–B1–B2 60.7(1), B1'–B2–B1 58.7(2), B2–C1–B1 70.5(2), B1–C2–B1' 68.5(2). (symmetry operation for ' : $x, 1/2 - y, z$; for '' : $-x, -y, 1 - z$; for # : $-x, y - 1/2, 1 - z$)

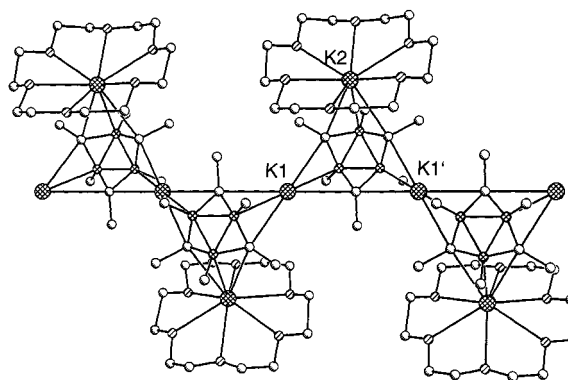


Figure 7. Structure of $[3(\text{K}^+)(\text{K}[18]\text{crown-6})^+]_m$ in the crystal showing segments of the polymer chain

increase. For a comparison with the structures of other organoalkali metal compounds see ref.^[8]

NMR spectroscopic Characterization

Two broad ^1H NMR signals at $\delta = -3.2$ and -3.4 are assigned to the methine protons of the initial reduction product $\{3[(\text{Li}^+)_2(\text{thf})_{2n}]\}_m$ in $[\text{D}_8]\text{THF}$ solution. Since the reduction yielded a mixture of diastereomers with different axial/equatorial C–Me orientations, three B–Me and two C–Me signals were found. This had already been observed by NMR spectroscopy and by X-ray crystal analysis for $(\text{MeCH})_3(\text{ClB})_3$, the precursor of **2**.^[5] The ^{11}B NMR signal of reduced **2** at $\delta = -29.2$ is at extremely high-field (neutral **2**: $\delta = 84.3$), and indicates the increased connectivity of the boron atoms.

The NMR signals could be assigned to a mixture of two diastereomers — one form with all the methine protons in axial configurations and the other with one equatorial and two axial methine protons. The ratio of diastereomers varies, but the all-axial form always dominates.

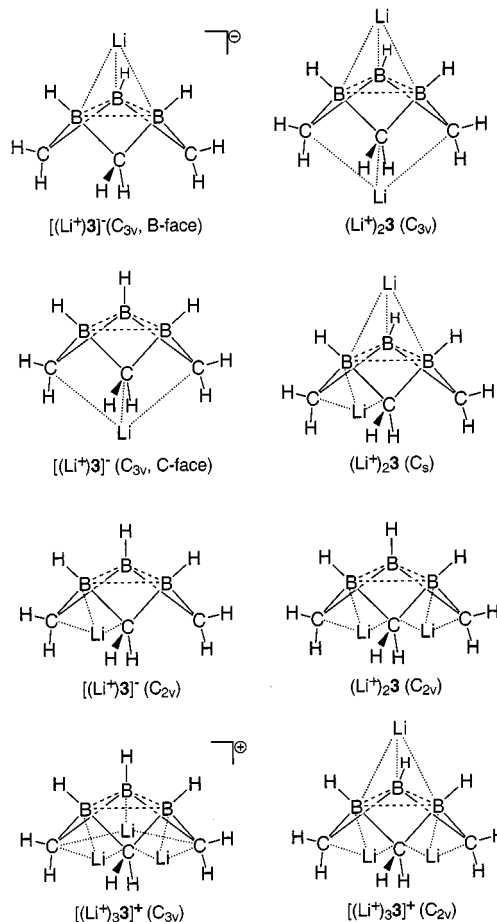
The reduction products show a pronounced high-field shift in their ^{11}B NMR spectra (Table 1), although there are quantitative differences showing two trends of opposite direction. The ^{11}B NMR chemical shifts decrease monotonously in absolute value within the alkali metal group, but only from Na to Cs, from $\delta = -35.3$ for $\{3[(\text{Na}^+)_{2}(\text{thf})_{2n}]\}_m$ to $\delta = -29.8$ for $\{3[(\text{Cs}^+)_{2}(\text{thf})_{2n}]\}_m$; the Li-reduced product $\{3[(\text{Li}^+)_{2}(\text{thf})_{2n}]\}_m$ ($\delta = -29.2$) does not seem to fit this trend. The same ordering occurs in the ^{13}C NMR spectra for the C–Me groups and the methine carbon atoms, again with $\{3[(\text{Li}^+)_{2}(\text{thf})_{2n}]\}_m$ as the exception. In contrast the ^1H NMR spectra show a trend to higher-field methine proton chemical shifts.

The special behavior of the Li-reduced species can be attributed to the decreased electronegativity (EN) of lithium.^[9,10] This is due to the smaller effective charge of the Li nucleus. From sodium to cesium the EN decreases monotonously and the C–H and C–Me proton shifts appear at increasingly higher fields (see Table 1).

Computational Results

IGLO ^{11}B NMR shift calculations^[7,11] of the C_{3v} model of $[(\text{CH}_2)_3(\text{BH})_3\text{Li}_3]^+ \{[(\text{Li}^+)_{3}\text{3}]\}^+$ gave $\delta^{11}_{\text{B}} = -31.8$, in very good agreement with the experimental value. The NICS values,^[7] $\delta = -28.5$ at the center of all the C and B atoms and $\delta = -42.3$ at the center of the three boron atoms, also indicate pronounced homoaromatic character (see below). Comprehensive computations on the various possible monomeric minima $[(\text{CH}_2)_3(\text{BH})_3\text{Li}_3]^+ \{[(\text{Li}^+)_{3}\text{3}]\}^+$, $(\text{CH}_2)_3(\text{BH})_3\text{Li}_2 \{[(\text{Li}^+)_{2}\text{3}]\}$ and $[(\text{CH}_2)_3(\text{BH})_3\text{Li}]^- \{[(\text{Li}^+)\text{3}]\}^-$, reveal that Li attachment at the B_3 face is preferred over a C_2B unit in all cases $\{[(\text{Li}^+)\text{3}]\}^-$: C_{3v} (B-face); $[(\text{Li}^+)_{2}\text{3}]\}^-$: C_s ; $[(\text{Li}^+)_{3}\text{3}]\}^+$: C_{2v} . The lithium bonding is predominantly electrostatic, but small covalent contributions to the interactions between the Li^+

centers and nearby H, B and C atoms are present. The C_2B -face coordination observed experimentally for $\{3[(\text{Li}^+)[\text{Li}(\text{thp})_2]^+]\}_4$ and $\{3[(\text{Li}^+)[(\text{Li}[12]\text{cr-4})_2]^+]\}_4$ may be attributed to the combined effects of the steric influences of the methyl groups at the B_3 face and to the electrostatic advantages of the tetrameric association.



Most surprising is the remarkable homoaromatic stabilization energy^[3] of the $[(\text{CH}_2)_3(\text{BH})_3]^{2-}$ dianion (**3**, $\text{R} =$

Table 1. NMR chemical shifts of reduced **2**, depending on the alkali metal

	Li	Na	K	Rb	Cs
^{11}B	-29.2	-35.3, -37.1	-32.4	-31.5	-29.8
^1H					
$(\text{CH}_3\text{CH}_{\text{ax}})_3$	-3.42 (m)	-3.34 (q)	-3.64 (q)	-3.78 (q)	-3.89 (q)
$(\text{CH}_3\text{CH}_{\text{ax}})_2$	-3.23 (m)	-3.03 (q)	-3.34 (q)	-3.46 (q)	-3.64 (q)
$(\text{CH}_3\text{CH}_{\text{ax}})_1$	-1.66 (m)	-1.57 (q)	-1.80 (q)	-1.84 (q)	-1.89 (q)
BCH_3	-0.59 (s, br)	-0.59 (s, br)	-0.71 (s, br)	-0.73 (s, br)	-0.76 (s, br)
BCH_3	-0.52 (s, br)		-0.65 (s, br)	-0.64 (s, br)	-0.72 (s, br)
$\text{CHCH}_3(\text{ax})$	0.81 (d)	0.82 (d)	0.82 (d)	0.84 (d)	0.82 (d)
$\text{CHCH}_3(\text{eq})$	1.23 (d)	1.05 (d)	1.03 (d)	0.93 (d)	0.91 (d)
$\text{CHCH}_3(\text{eq})$	1.35 (d)	1.16 (d)	1.09 (d)	1.05 (d)	1.01 (d)
^{13}C					
CHCH_3	15.4	15.2	15.5	16.1	16.1
CHCH_3	-4.0	-3.9	-2.1	-1.3	-1.3
BCH_3	15.6	15.4	16.0	17.8	17.8

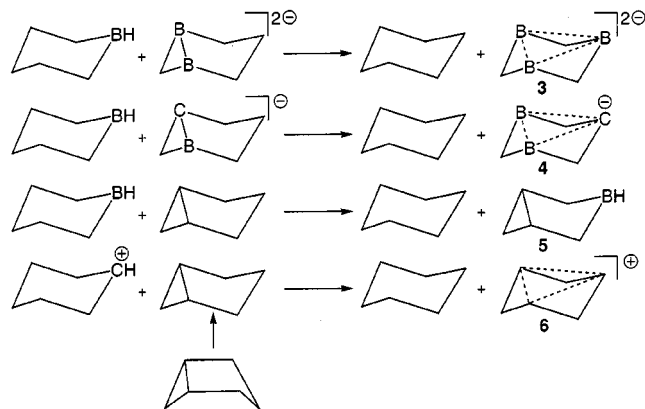
Table 2. Stabilization energies (kcalmol⁻¹ at //B3LYP/6-311+G**) and NICS values (at PW91/IGLO III)^[4] for the trishomoaromatic systems 3–6

Trishomoaromatic system	Isodesmic reaction ^[a]	vs. boat form ^[b]	NICS(0) ^[c]	NICS(rc) ^[d]
[(CH ₂) ₃ (BH) ₃] ²⁻ (3)	-41.05	-32.35	-35.4	-22.5
[(CH ₂) ₃ (CH)(BH) ₂] ⁻ (4)	-19.63	-16.11	-37.1	-21.4
[(CH ₂) ₃ (CH) ₂ (BH)] (5)	+5.55	+6.55	-34.8	-16.7
[(CH ₂) ₃ (CH) ₃] ⁺ (6)	-8.73	-12.54	-46.4	-22.7

^[a] The isodesmic equations (Scheme 5) involve cyclohexane and 3–6 as product pairs. The reactants are cyclohexyl cation (for **6**) and boracyclohexane (for 3–5), as well as bicyclo[3.1.0]hexane (for **5** and **6**) and its 1-(B⁻) (for **4**) and 1,5-(B⁻)₂ (for **3**) counterparts. – ^[b] Energy differences between 3–6 and their boat-form conformers which lack 3c,2e bonding (see ref.^[17] for a prior use of this method). –

^[c] Computed at the mass unweighted centers of the 6-rings. – ^[d] The ring current contributions (localized by the IGLO method) computed at the centers of the three C/B atom triangles involved in 3c,2e bonding.

R' = H), which is larger than all three of the isoelectronic counterparts 4–6 (Table 2), even when evaluated by two different methods.^[12] These stabilization energies are based on the isodesmic reactions in Scheme 5 and the chair (delocalized)–boat (localized) energy differences. This is caused by the reduced coulombic interaction between the two negative charges when they are delocalized over the B₃ triangle. In contrast, the electron repulsion in the classic reference species is high because of two adjacent B⁻ units. The positive stabilization energies of the neutral analog **5** reflect the ring strain required to achieve the chair conformation (which is greater than the stabilization to be gained). This situation is discussed in ref.^[12] The NICS(0) values, based on total NMR shieldings in the six-membered ring centers, and the NICS(rc) values in the 3c,2e ring centers (also given in Table 2) measure the current contributions. Malkin's implementation^[7b] of Kutzelnigg's IGLO program^[11] provides a detailed breakdown of the total shieldings in terms of all the localized orbital contributions.



Scheme 5

Of greatest interest are the diatropic effects due to the cyclic electron delocalization [i.e., the magnetic evaluation of the 3c,2e “aromatic” bonding given by NICS(rc)]. These values are augmented by the local diatropic shielding contributions of nearby C–C, C–H and B–H bonds. Hence, the NICS(0) values are displaced further upfield. (The local induced circulations of the sigma C–C bonds in benzene,

in contrast, are paratropic and reduce the NICS(0) value to ca -10.) The benzene NICS(rc, i.e. π) of about -22 at the ring center is quite similar to the 3c,2e data above.

Conclusion

The reaction of **2** with lithium gave tetrameric aggregates of the trishomoaromatic compounds {3(Li⁺)[Li(thp)₂]⁺}₄ and [3(Li⁺)₄{Li([12]cr-4)₂]⁺}]₄ in the solid state. The expected monomeric dianion **3** (R = R' = Me) and the cation 3[(Li⁺)(thf)₂]₃⁺ as electronic analogues to the trishomocyclopropenyl cation **6**^[6] could not be isolated. Alternatively, the monomeric unit 3[(Li⁺)(thf)₂]₃⁺, with two donor molecules at each of the three Li centers, may be described as a hypho cluster with 26 skeleton electrons.^[13]

The reduction product of **2** with sodium crystallizes as a polymeric, meander-like chain, in which the trishomoaromatic units are bridged at C₂B faces by half of the sodium ions, with the other half connected in terminal positions to one C₂B face and three THF ligands. A tetramer of **3** with an unusual structure was obtained in the presence of [18]crown-6. The linear polymer [3(K⁺)(K[18]cr-6)⁺]_m is formed with potassium as the electron donor. NMR spectroscopic data show that reduction with rubidium and with cesium also led to the doubly reduced ring systems.

The NMR spectra of all the Li-reduced compound {3[(M⁺)₂(thf)_{2n}]_m} show regular trends of chemical shifts from Na to Cs, but the Li values are often out of line due to the exceptional electronegativity of lithium. The trishomoaromatic delocalized three center, two electron bonding in the reduced 1,3,5-triboracyclohexanes (**3**), as well as in the isoelectronic series 3–5, is demonstrated by the highly negative NICS values computed inside the rings. These indicate the presence of large induced diatropic ring currents in all these systems. In addition, the stabilization energies due to the 3c,2e delocalization are quite large.

Experimental Section

General: All reactions were carried out under dry argon or nitrogen using standard Schlenk techniques. Solvents were dried, distilled,

and saturated with nitrogen. Glassware was dried with a heat-gun under high vacuum. The alkali metals were washed with *n*-hexane and THF, heated in THF for 2 h under reflux and filtered. Lithium was used as a powder, and sodium, potassium, rubidium and cesium as blocks. — ^1H , ^{13}C and ^{11}B NMR: Bruker DRX 200 spectrometer, NMR references are $(\text{CH}_3)_4\text{Si}$ and $\text{Et}_2\text{O}\cdot\text{BF}_3$.

General Procedure for the Reduction of the Triboraheterocycles: A suspension of excess alkali metal in THF or Et_2O was cooled to 0 °C. The boron heterocycle was added and stirred overnight while warming to room temperature. Separation of the unreacted alkali metal by filtration through a glass filter of G III porosity led to clear yellow-orange solutions. Removal of the solvent gave amorphous residues of $[\mathbf{3}(\text{M}^+)_2(\text{thf})_2]_{\text{m}}$ and $[\mathbf{3}(\text{M}^+)_2(\text{OEt})_2]_{\text{m}}$, which are soluble in $[\text{D}_8]\text{THF}$.

Reduction of 2 with Lithium: Amounts: diethyl ether (20 mL), **2** (200 mg, 1.23 mmol). For crystallization the solution was concentrated to 1–2 mL by vacuum evaporation and THP or $[\mathbf{12}]\text{crown-4}$ (0.2 mL) was added to yield $[\mathbf{3}(\text{Li}^+)_4[\text{Li}(\text{thp})_2]_4]$ (28 mg, 7%) or $[\mathbf{3}(\text{Li}^+)_4\{\text{Li}([\mathbf{12}]\text{cr-4})_2\}_4]$ (12 mg, 3%). NMR spectroscopic data of the initial reduction product $[\mathbf{3}(\text{Li}^+)_2(\text{OEt})_2]_{\text{m}}$: ^1H NMR (200 MHz, $[\text{D}_8]\text{THF}$): $\delta = -3.42$ [q, $^3J(\text{H,H}) = 3$ Hz, 3 H, CH_{ax}], -3.2 (br. m, 2 H, CH_{ax}), -1.7 (br. m, 1 H, CH_{eq}), -0.6 (br. s, 9 H, BCH_3), -0.5 (br. s, 6 H, BCH_3), -0.5 (br. s, 3 H, BCH_3), 0.81 [d, $^3J(\text{H,H}) = 3$ Hz, 3 H, $\text{C}(\text{CH}_3)_{\text{ax}}$], 1.23 [d, $^3J(\text{H,H}) = 3$ Hz, 6 H, $\text{C}(\text{CH}_3)_{\text{eq}}$], 1.35 [d, $^3J(\text{H,H}) = 3$ Hz, 9 H, $\text{C}(\text{CH}_3)_{\text{eq}}$]. — ^{13}C NMR (50 MHz, $[\text{D}_8]\text{THF}$): $\delta = -4.0$ (CH), 15.4 (CCH_3), 15.6 (BCH_3). — ^{11}B NMR (64 MHz, $[\text{D}_8]\text{THF}$): $\delta = -29.2$.

Reduction of 2 with Sodium: Amounts: THF (40 mL), **2** (150 mg, 0.93 mmol). Crystallization from the filtered solution after solvent

removal to ca. 1 mL gave $\{\mathbf{3}(\text{Na}^+)[\text{Na}(\text{thf})_3]^+\}_{\text{m}}$ (95 mg, 0.22 mmol, 24%). After addition of $[\mathbf{18}]\text{crown-6}$ (420 mg) to the filtered solution, crystallization occurred after solvent evaporation to 1 mL to give $\{(\text{thf})_2\text{Na}([\mathbf{18}]\text{cr-6})^+\}[\mathbf{3}(\text{Na}^+)(\text{thf})_4(\text{Na}^+)_2]^{2-}\{(\text{thf})\text{Na}([\mathbf{18}]\text{cr-6})^+\}$ (43 mg, 0.02 mmol, 9%). NMR spectroscopic data of the initial reduction product $[\mathbf{3}(\text{Na}^+)_2(\text{thf})_2]_{\text{m}}$ (ratio of diastereomers $(\text{CH}_{\text{ax}})_3/(\text{CH}_{\text{ax}})_2(\text{CH}_{\text{eq}}) = 3:1$): ^1H NMR (200 MHz, $[\text{D}_8]\text{THF}$): $\delta = -3.34$ [q, $^3J(\text{H,H}) = 3$ Hz, 3 H, CH_{ax}], -3.03 [q, $^3J(\text{H,H}) = 3$ Hz, 2 H, CH_{ax}], -1.57 [q, $^3J(\text{H,H}) = 3$ Hz, 1 H, CH_{eq}], -0.6 (br. s, 9 H, BCH_3), 0.82 [d, $^3J(\text{H,H}) = 3$ Hz, 3 H, $\text{C}(\text{CH}_3)_{\text{ax}}$], 1.05 [d, $^3J(\text{H,H}) = 3$ Hz, 6 H, $\text{C}(\text{CH}_3)_{\text{eq}}$], 1.16 [d, $^3J(\text{H,H}) = 3$ Hz, 9 H, $\text{C}(\text{CH}_3)_{\text{eq}}$]. — ^{13}C NMR (50 MHz, $[\text{D}_8]\text{THF}$): $\delta = -3.9$ (CH), 15.2 (CCH_3), 15.4 (BCH_3). — ^{11}B NMR (64 MHz, $[\text{D}_8]\text{THF}$): $\delta = -35.3$ and -37.1 .

Reduction of 2 with Potassium: Amounts: THF (40 mL), **2** (140 mg, 0.86 mmol). After reaction and filtration, $[\mathbf{18}]\text{crown-6}$ (350 mg) was added to the solution. The solvent was partially removed in vacuum and $[\mathbf{3}(\text{K}^+)(\text{K}[\mathbf{18}]\text{cr-6})^+]_{\text{m}}$ (56 mg, 0.11 mmol, 12%) crystallized. NMR spectroscopic data of the initial reduction product $[\mathbf{3}(\text{K}^+)_2(\text{thf})_2]_{\text{m}}$ (ratio of diastereomers $(\text{CH}_{\text{ax}})_3/(\text{CH}_{\text{ax}})_2(\text{CH}_{\text{eq}}) = 6:1$): ^1H NMR (200 MHz, $[\text{D}_8]\text{THF}$): $\delta = -3.64$ [q, $^3J(\text{H,H}) = 3$ Hz, 3 H, CH_{ax}], -3.34 [q, $^3J(\text{H,H}) = 3$ Hz, 2 H, CH_{ax}], -1.80 [q, $^3J(\text{H,H}) = 3$ Hz, 1 H, CH_{eq}], -0.7 (br. s, 9 H, BCH_3), -0.6 (br. s, 6 H, BCH_3), 0.82 [m, 3 H, $\text{C}(\text{CH}_3)_{\text{ax}}$], 1.03 [d, $^3J(\text{H,H}) = 3$ Hz, 6 H, $\text{C}(\text{CH}_3)_{\text{eq}}$], 1.09 [d, $^3J(\text{H,H}) = 3$ Hz, 9 H, $\text{C}(\text{CH}_3)_{\text{eq}}$]. — ^{13}C NMR (50 MHz, $[\text{D}_8]\text{THF}$): $\delta = -2.1$ (CH), 15.5 (CCH_3), 16.0 (BCH_3). — ^{11}B NMR (64 MHz, $[\text{D}_8]\text{THF}$): $\delta = -32.4$.

Reduction of 2 with Rubidium: Amounts: THF (50 mL), **2** (200 mg, 1.23 mmol). NMR spectroscopic data of the amorphous reduction

Table 3. Crystal data and structure refinement of $\{\mathbf{3}(\text{Li}^+)[\text{Li}(\text{thp})_2]_4\}$, $\{\mathbf{3}(\text{Li}^+)_2([\mathbf{12}]\text{cr-4})_2\}_4$, $\{\mathbf{3}(\text{Na}^+)[\text{Na}(\text{thf})_3]^+\}_{\text{m}}$, $\{(\text{thf})_2\text{Na}([\mathbf{18}]\text{cr-6})^+\}[\mathbf{3}(\text{Na}^+)(\text{thf})_4(\text{Na}^+)_2]^{2-}\{(\text{thf})\text{Na}([\mathbf{18}]\text{cr-6})^+\}$ and $[\mathbf{3}(\text{K}^+)(\text{K}[\mathbf{18}]\text{crown-6})^+]_{\text{m}}$

	$\{\mathbf{3}(\text{Li}^+)_4[\text{Li}([\mathbf{12}]\text{cr-4})_2]_4\}$	$\{\mathbf{3}(\text{Na}^+)[\text{Na}(\text{thf})_3]^+\}_{\text{m}}$	Octahedral Na_6 compd. (Fig. 4) ^[a]	$[\mathbf{3}(\text{K}^+)(\text{K}[\mathbf{18}]\text{cr-6})^+]_{\text{m}}$
Empirical formula	$\text{C}_{25}\text{H}_{53}\text{B}_3\text{Li}_2\text{O}_8$	$\text{C}_{21}\text{H}_{45}\text{B}_3\text{Na}_2\text{O}_3$	$\text{C}_{96}\text{H}_{204}\text{B}_{12}\text{Na}_8\text{O}_{21}$	$\text{C}_{29}\text{H}_{61}\text{B}_3\text{K}_2\text{O}_8$
Molecular weight	527.98	423.98	2008.23	648.41
Crystal system	Tetragonal	Orthorhombic	Orthorhombic	Monoclinic
Space group	$P4_2/n$	$P2_12_12_1$	$Pnmm$	$P2_1/m$
<i>a</i> [Å]	20.156(11)	11.0551(3)	22.142(5)	11.746(2)
<i>b</i> [Å]	20.156(11)	15.9133(4)	28.468(5)	11.372(2)
<i>c</i> [Å]	14.937(8)	29.9410(8)	19.154(3)	13.988(2)
α [°]	90	90	90	90
β [°]	90	90	90	97.37(1)
γ [°]	90	90	90	90
<i>V</i> [Å ³]	6068(6)	5267.3(2)	12073(4)	1853.0(5)
<i>Z</i>	8	8	4	2
Calcd. density [g/cm ³]	1.156	1.07	1.11	1.16
Absorp. coeff. [mm ⁻¹]	0.080	0.09	0.10	0.30
<i>F</i> (000)	2304	1856	4384	704
Crystal size [mm]	0.80 × 0.50 × 0.35	0.32 × 0.44 × 0.45	0.15 × 0.15 × 0.25	0.09 × 0.35 × 0.46
Θ_{max} [°]	25.1	25.1	18.0	28.3
Index ranges	0/23, 0/23, 0/17	−13/13, 0/18, 0/35	0/19, 0/24, 0/16	−14/15, −12/15, −18/18
Unique reflections	5341	9324	4331	4688
Observed [<i>I</i> > 2σ(<i>I</i>)]	2790	6794	2469	3700
Parameters	364	544	407	299
Final <i>R</i> indices				
<i>R</i> 1 [<i>I</i> > 2σ(<i>I</i>)]	0.060	0.088	0.117	0.071
<i>wR</i> 2	0.141	0.265	0.356	0.218
Largest diff. peak/hole [e/Å ³]	0.191/−0.185	0.61/−0.26	0.61/−0.63	0.89/−0.68

^[a] $\{(\text{thf})_2\text{Na}([\mathbf{18}]\text{cr-6})^+\}[\mathbf{3}(\text{Na}^+)(\text{thf})_4(\text{Na}^+)_2]^{2-}\{(\text{thf})\text{Na}([\mathbf{18}]\text{cr-6})^+\}$.

product $[3(\text{Rb}^+)_2(\text{THF})_{2n}]_m$ (ratio of diastereomers $(\text{CH}_{\text{ax}})_3/(\text{CH}_{\text{ax}})_2(\text{CH}_{\text{eq}}) = 9:1$): ^1H NMR (200 MHz, $[\text{D}_8]\text{THF}$): $\delta = -3.78$ [q, $^3J(\text{H,H}) = 3$ Hz, 3 H, CH_{ax}], -3.46 [q, $^3J(\text{H,H}) = 3$ Hz, 2 H, CH_{ax}], -1.84 [q, $^3J(\text{H,H}) = 3$ Hz, 1 H, CH_{eq}], -0.7 (br. s, 9 H, BCH_3), -0.6 (br. s, 6 H, BCH_3), 0.84 [m, 3 H, $\text{C}(\text{CH}_3)_{\text{ax}}$], 0.93 [d, $^3J(\text{H,H}) = 3$ Hz, 6 H, $\text{C}(\text{CH}_3)_{\text{eq}}$], 1.05 [d, $^3J(\text{H,H}) = 3$ Hz, 12 H, $\text{C}(\text{CH}_3)_{\text{eq}}$]. ^{13}C NMR (50 MHz, $[\text{D}_8]\text{THF}$): $\delta = -1.3$ (CH), 16.1 (CCH_3), 17.8 (BCH_3). ^{11}B NMR (64 MHz, $[\text{D}_8]\text{THF}$): $\delta = -31.5$.

Reduction of 2 with Cesium: Amounts: THF (50 mL), **2** (190 mg, 1.17 mmol). NMR spectroscopic data of the amorphous reduction product $[3(\text{Cs}^+)_2(\text{THF})_{2n}]_m$ (ratio of diastereomers $(\text{CH}_{\text{ax}})_3/(\text{CH}_{\text{ax}})_2(\text{CH}_{\text{eq}}) = 12:1$): ^1H NMR (200 MHz, $[\text{D}_8]\text{THF}$): $\delta = -3.89$ [q, $^3J(\text{H,H}) = 3$ Hz, 3 H, CH_{ax}], -3.64 [q, $^3J(\text{H,H}) = 3$ Hz, 2 H, CH_{ax}], -1.89 [q, $^3J(\text{H,H}) = 3$ Hz, 1 H, CH_{eq}], -0.8 (br. s, 9 H, BCH_3), -0.7 (br. s, 6 H, BCH_3), 0.82 [d, $^3J(\text{H,H}) = 3$ Hz, 3 H, $\text{C}(\text{CH}_3)_{\text{ax}}$], 0.91 [d, $^3J(\text{H,H}) = 3$ Hz, 6 H, $\text{C}(\text{CH}_3)_{\text{eq}}$], 1.01 [d, $^3J(\text{H,H}) = 3$ Hz, 9 H, $\text{C}(\text{CH}_3)_{\text{eq}}$]. ^{13}C NMR (50 MHz, $[\text{D}_8]\text{THF}$): $\delta = -1.3$ (CH), 16.1 (CCH_3), 17.8 (BCH_3). ^{11}B NMR (64 MHz, $[\text{D}_8]\text{THF}$): $\delta = -29.8$.

X-ray Structure Determinations of $\{3(\text{Li}^+)[\text{Li}(\text{thp})_2]^+\}_4$, $\{3(\text{Li}^+)_4[\text{Li}(\text{12cr-4})_2]^+\}_4$, $\{3(\text{Na}^+)[\text{Na}(\text{thf})_3]^+\}_m$, $\{(\text{thf})_2\text{-Na}(\text{18cr-6})\}^+ \{3(\text{Na}^+)(\text{thf})_4(\text{Na}^+)_2\}^{2-} \{(\text{thf})\text{Na}(\text{18cr-6})\}^+$ and $\{3(\text{K}^+)[\text{K}(\text{18cr-6})]^+\}_m$: Crystal data and details of the structure determinations are listed in Table 3. Intensity data for $\{3(\text{Li}^+)[\text{Li}(\text{thp})_2]^+\}_4$ and $\{3(\text{Li}^+)_4[\text{Li}(\text{12cr-4})_2]^+\}_4$ were collected at 210 K with a Siemens Stoe AED2 diffractometer, and for $\{3(\text{Na}^+)[\text{Na}(\text{thf})_3]^+\}_m$, $\{(\text{thf})_2\text{Na}(\text{18cr-6})\}^+ \{3(\text{Na}^+)(\text{thf})_4(\text{Na}^+)_2\}^{2-} \{(\text{thf})\text{Na}(\text{18cr-6})\}^+$ and $\{3(\text{K}^+)[\text{K}(\text{18cr-6})]^+\}_m$ at 173 K with a Bruker AXS Smart 1000 (Mo- K_α radiation, $\lambda = 0.71073$ Å, graphite monochromator, ω -scan). The structures were solved by direct methods and refined by least-squares methods based on F^2 with all measured reflections (SHELXL-97).^[14] Non-hydrogen atoms were refined anisotropically (in $\{(\text{thf})_2\text{Na}(\text{18cr-6})\}^+ \{3(\text{Na}^+)(\text{thf})_4(\text{Na}^+)_2\}^{2-} \{(\text{thf})\text{Na}(\text{18cr-6})\}^+$ only the Na atoms). Most of the hydrogen atoms were inserted in their calculated positions. The THF and crown ligands are in some cases severely disordered. The crystal structure of $\{(\text{thf})_2\text{Na}(\text{18cr-6})\}^+ \{3(\text{Na}^+)(\text{thf})_4(\text{Na}^+)_2\}^{2-} \{(\text{thf})\text{Na}(\text{18cr-6})\}^+$ is not very precise, due to the very limited data set.

Crystallographic data (excluding structure factors) for the structures reported in this paper have been deposited with the Cambridge Crystallographic Data Center as supplementary publication nos. CCDC-133326 ($\{3(\text{Li}^+)_2[\text{Li}(\text{12cr-4})_2]^+\}_4$), -156933 ($\{3(\text{Na}^+)[\text{Na}(\text{thf})_3]^+\}_m$), -156934 ($\{(\text{thf})_2\text{Na}(\text{18cr-6})\}^+ \{3(\text{Na}^+)(\text{thf})_4(\text{Na}^+)_2\}^{2-} \{(\text{thf})\text{Na}(\text{18cr-6})\}^+$) and -156935 ($\{3(\text{K}^+)[\text{K}(\text{18cr-6})]^+\}_m$). Copies of the data can be obtained free of charge upon application to CCDC, 12 Union Road, Cambridge CB2 1EZ, UK [Fax: (internat.) +44-1223/336-033; E-mail: deposit@ccdc.cam.ac.uk].

Acknowledgments

This work was supported by the Deutsche Forschungsgemeinschaft (Schwerpunkt Polyeder) and the Fonds der Chemischen Industrie.

- [1] G. E. Herberich, in *Comprehensive Organometallic Chemistry* (Eds. G. Wilkinson, F. G. A. Stone, E. W. Abel), Pergamon Press **1982**, vol. 1, pp. 381–408.
- [2] M. Unverzagt, G. Subramanian, M. Hofmann, P. v. R. Schleyer, S. Berger, K. Harms, W. Massa, A. Berndt, *Angew. Chem.* **1997**, *109*, 1567–1568; *Angew. Chem. Int. Ed. Engl.* **1997**, *36*, 1469–1472.
- [3] D. Scheschke, A. Ghaffari, P. Amseis, M. Unverzagt, G. Subramanian, M. Hofmann, P. v. R. Schleyer, H. F. Schaefer III, G. Geiseler, W. Massa, A. Berndt, *Angew. Chem.* **2000**, *112*, 1329–1333; *Angew. Chem. Int. Ed.* **2000**, *39*, 1272–1276.
- [4] W. Löbblin, H. Pritzkow, P. von R. Schleyer, L. R. Schmitz, W. Siebert, *Angew. Chem.* **2000**, *112*, 1333–1336; *Angew. Chem. Int. Ed.* **2000**, *39*, 1276–1280.
- [5] T. Deforth, M. Kaschke, H. Stock, H. Pritzkow, W. Siebert, *Z. Naturforsch.* **1997**, *52b*, 823–830.
- [6] [6a] S. Winstein, J. Sonnenberg, L. de Vries, *J. Am. Chem. Soc.* **1959**, *81*, 6523–6524. – [6b] S. Winstein, *J. Am. Chem. Soc.* **1959**, *81*, 6524–6525. – [6c] S. Masamune, M. Sakai, A. V. Kemp-Jones, T. Nakashima, *Can. J. Chem.* **1974**, *52*, 855–857. – [6d] K. J. Szabo, E. Kraka, D. Cremer, *J. Org. Chem.* **1996**, *61*, 2783–2800.
- [7] [7a] P. v. R. Schleyer, C. Maerker, A. Dransfeld, H. Jiao, N. J. R. van Eikema Hommes, *J. Am. Chem. Soc.* **1996**, *118*, 6317–6318. – [7b] P. v. R. Schleyer, H. Jiao, N. J. R. van Eikema Hommes, V. G. Malkin, O. L. Malkina, *J. Am. Chem. Soc.* **1997**, *119*, 12669–12670. – [7c] P. v. R. Schleyer, G. Subramanian, H. Jiao, K. Najafian, M. Hofmann, in *Advances in Boron Chemistry* (Ed.: W. Siebert), The Royal Society of Chemistry, Cambridge, UK, **1997**, pp. 3–14. – [7d] P. v. R. Schleyer, K. Najafian, *Inorg. Chem.* **1998**, *37*, 3454–3470. – [7e] P. v. R. Schleyer, K. Najafian, A. M. Mebel, *Inorg. Chem.* **1998**, *37*, 6765–6772. – [7f] M. Hofmann, D. Scheschke, A. Ghaffari, G. Geiseler, W. Massa, H. F. Schaefer, A. Berndt, *J. Mol. Model.*, submitted.
- [8] [8a] M. Geissler, J. Kopf, B. Schubert, E. Weiss, W. Neugebauer, P. v. R. Schleyer, *Angew. Chem.* **1987**, *99*, 569–570. – [8b] C. Schade, P. v. R. Schleyer, M. Geissler, E. Weiss, *Angew. Chem.* **1986**, *98*, 922–924; *Angew. Chem. Int. Ed. Engl.* **1986**, *25*, 902–904. – [8c] C. Schade, P. v. R. Schleyer, *Adv. Organomet. Chem.* **1987**, *27*, 169–278.
- [9] C. Lambert, P. v. R. Schleyer, *Angew. Chem.* **1994**, *106*, 1187–1199; *Angew. Chem. Int. Ed. Engl.* **1994**, *33*, 1129–1140.
- [10] C. Lambert, M. Kaupp, P. v. R. Schleyer, *Organometallics* **1993**, *12*, 853–859.
- [11] W. Kutzelnigg, U. Fleischer, M. Schindler, in *NMR: Basic Principles and Progress*, Springer Verlag Berlin, **1990**, Vol. 23, 165.
- [12] J. M. Schulman, R. L. Disch, P. v. R. Schleyer, M. Bühl, M. Bremer, W. Koch, *J. Am. Chem. Soc.* **1992**, *114*, 7897–7901.
- [13] [13a] K. Wade, *Adv. Inorg. Chem. Radiochem.* **1976**, *18*, 1–66. – [13b] D. M. P. Mingos, *Adv. Organomet. Chem.* **1977**, *15*, 1–51.
- [14] G. M. Sheldrick, SHELXTL NT5.10, Bruker AXS, Madison, WI., **1999**.

Received January 17, 2001
[101022]